

Stereochemical Studies on Sphinxolide: Advances in the *J*-Based NMR Determination of the Relative Configuration of Flexible Systems

Carla Bassarello,^[a] Giuseppe Bifulco,^[a] Angela Zampella,^[b] Maria Valeria D'Auria,^[b] Raffaele Riccio,^[a] and Luigi Gomez-Paloma^{*[a]}

Dedicated to Professor Luigi Minale

Keywords: Structure elucidation / Natural products / NMR spectroscopy / Sphinxolide / Antitumor agents

An improved version of the *J*-based NMR configurational analysis of flexible organic molecules, that relies on extensive use of HSQC-TOCSY spectra, was applied to the stereochemical study of sphinxolide, a potent anti-tumor marine macrolide acting on cell microfilaments that has lately

proven to circumvent multi-drug-resistance (MDR) in cancer cells. NMR data allowed stereochemical assignment of all molecular segments except the C18–C19 unit, whose configuration had to be addressed by a chemical/degradative approach.

Introduction

Obtaining full stereochemical knowledge is a key step in the structural elucidation of complex organic molecules. This information becomes particularly crucial in the case of bioactive natural products (it is a prerequisite for undertaking their total synthesis), for conformational and structure activity relationship (SAR) studies, and for the interpretation of the molecular basis of their mode of action. The stereochemical analysis of flexible systems is usually a very challenging task due to the lack of information on the conformational behavior of the molecule that is being studied. In this context, methods of configurational analysis based

on NMR spectroscopy are particularly interesting because they allow the preservation of the (often limited) sample for biological and pharmacological assays.

In this communication, we present a stereochemical study on the marine natural product sphinxolide (**1**, see Figure 1 and text below).

Results and Discussion

Recently, Murata et al. reported a *J*-based NMR approach^[1] relying on extensive use of proton-carbon ^{2,3}*J* couplings, often in combination with NOE/ROE data. This approach allows the determination of the predominant rot-

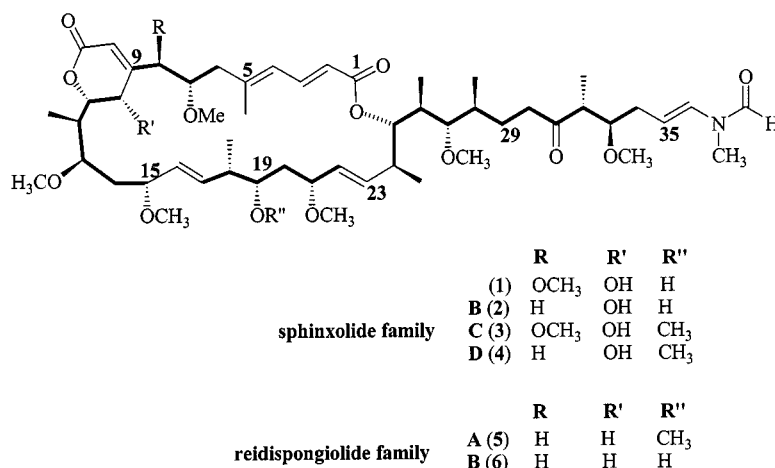


Figure 1. The sphinxolide and reidispongiolides families

^[a] Dipartimento di Scienze Farmaceutiche, Università di Salerno, Via Ponte Don Melillo, 84084 Fisciano (SA), Italy
Fax: (internat.) +39-089/962-828
E-mail: gomez@unisa.it

^[b] Dipartimento di Chimica delle Sostanze Naturali, Università di Napoli "Federico II", Via D. Montesano 49, 80131, Napoli, Italy

amer, with the correct relative configuration, among the six possible staggered conformers of each two-carbon fragment in which a chiral molecule with consecutive and alternating stereogenic centers can be ideally divided. However, the measurement of heteronuclear ^{2,3}*J* couplings at natural abundance is a rather difficult task due to the intrinsic low-

sensitivity of the NMR techniques involved. For instance, such couplings can be accurately extracted from ω_1 -half-filtered TOCSY (HETLOC) spectra^[2] by measuring the ω_2 -displacement of proton multiplets. Although very informative, the HETLOC technique requires, for 500–600 MHz spectrometers, samples with a concentration around 10 mM or even greater. In addition, the measurement of proton-carbon coupling constant values in HETLOC spectra can be complicated by the occurrence of severe signal overlapping, as is often observed in the crowded 1D and 2D proton spectra of complex natural products. Phase-sensitive (PS) HMBC spectra^[3,4] have also been used for extracting these coupling constants through relative measurements of cross-peak volumes and proposed for this purpose in the Murata approach.^[1] This technique has the advantage of being much more sensitive (especially its pulse field gradient (PFG) enhanced version)^[5] and offers more effective spectral dispersion through the carbon ω_1 -dimension. However, this method needs an internal reference for a meaningful quantitative peak volume comparison (cf. the determination of interproton distances from NOESY peak volumes) and therefore requires the independent measurement of a number of heteronuclear coupling constants that, up until now, had to be obtained through HETLOC spectra. In any case, the application of this powerful methodology depends on the possibility of obtaining good HETLOC spectra. However, a PFG-enhanced version of the coupled/decoupled HSQC-TOCSY technique has also been used for the measurement of long-range heteronuclear couplings in conformational studies of biomolecules.^[6] In this case the $^{2,3}J_{\text{CH}}$ values are obtained by a computer-aided analysis of in-phase ^1H multiplets (derived from ω_2 -slices) with and without heteronuclear splitting. High quality HSQC-TOCSY spectra suitable for this purpose can be obtained at 500–600 MHz fields on 2–3 mm samples, a range of concentration for which HETLOC spectra have a very low signal-to-noise (S/N) ratio. Better results in terms of the S/N ratio can be achieved through the application of a sensitivity and gradient enhanced version of the HETLOC technique recently published by Köver et al.,^[7] although J_{CH} couplings cannot always be determined when severe cross-peak overlap is present in crowded spectral regions (see Figure 2).

This HSQC-TOCSY approach was used for the stereochemical study of sphinxolide (**1**) (see Figure 1),^[8,9] a potent anti-tumor marine 26-membered macrolide capable of specifically targeting cell microfilaments, causing their disruption, at nanomolar concentrations.^[10] This compound, like other related members of the sphinxolide and reidspongolide classes,^[11,12] also exhibits the ability to circumvent multi-drug resistance (MDR) in cancer cells, suggesting that compounds of this family may prove useful models for the development of new drugs for anti-cancer chemotherapy. The sphinxolide molecule features 17 stereogenic centers with still unknown configurations in a quite flexible carbon framework, due to the presence of a side chain and a large macrolactone ring, and is therefore a particularly interesting candidate for this J -based stereochem-

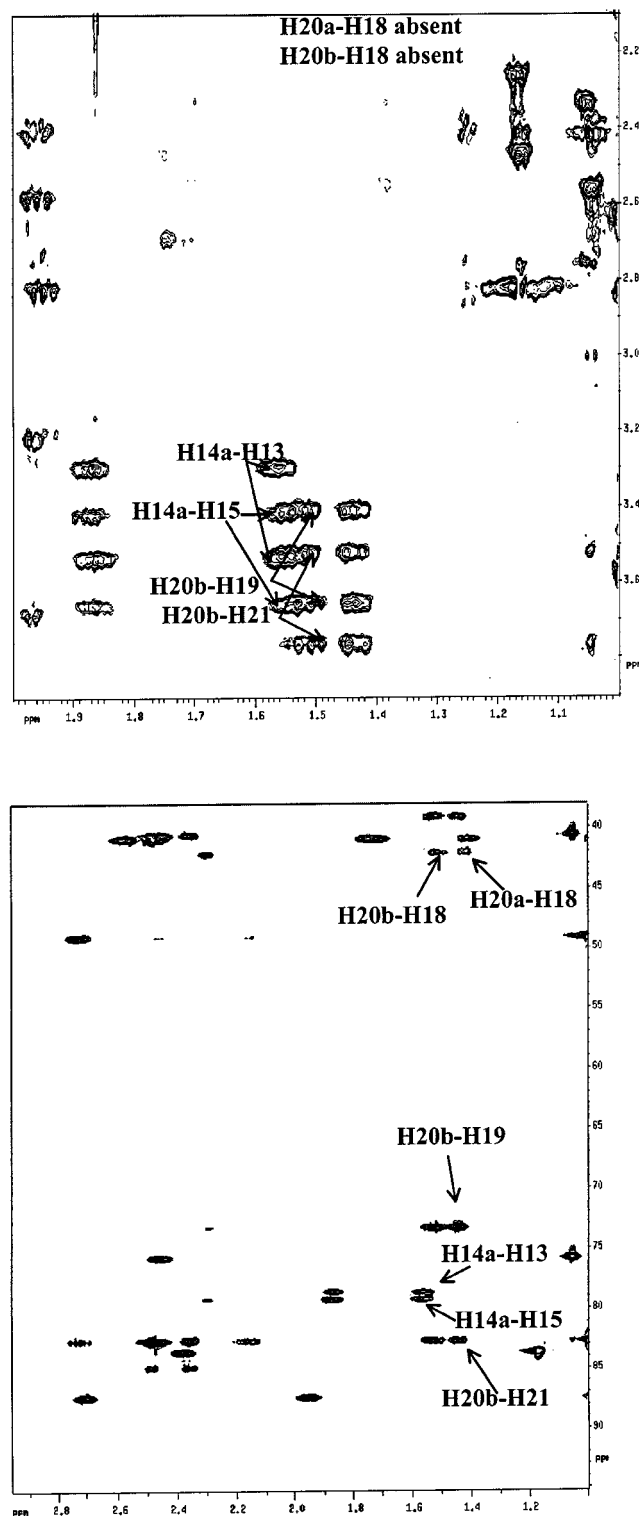


Figure 2. Expanded regions of PFG-HETLOC (top) and PFG-HSQC-TOCSY (bottom) spectra of sphinxolide at 600 MHz, showing the superior and convenient dispersion of signals in the ω_1 (^{13}C)-dimension that can be obtained by the HSQC-TOCSY technique

ical analysis. ^{13}C coupled and decoupled HSQC-TOCSY spectra were recorded on a 3 mm sample of sphinxolide (CDCl_3 , 600 MHz) at 276 and 300 K and the proton-carbon $^{2,3}J$ couplings were extracted through a computer-aided

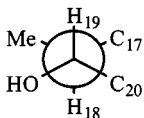
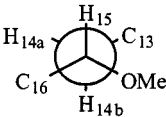
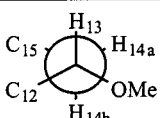
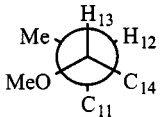
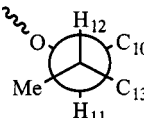
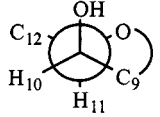
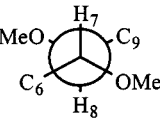
analysis of the heteronuclear coupled and decoupled multiplets acquired in two separate experiments, according to the method proposed by Köver et al.^[5] The advantage of the HSQC-TOCSY technique in resolving crowded spectral regions can be appreciated from a direct comparison of the HSQC-TOCSY and PFG-HETLOC spectra of sphinxolide (1) (Figure 2). In all, twelve heteronuclear couplings that could not be extracted from PFG-HETLOC spectra were measured with the aid of the HSQC-TOCSY technique. We then used all the $^{2,3}J_{CH}$ values obtained from HSQC-TOCSY spectra as a reference for the measurement of additional couplings in the PFG-PS-HMBC spectra. In this way we were able to overcome the main limitation of the HSQC-TOCSY technique, namely the possibility of observing long

range couplings only between protons and *protonated* (and not quaternary) carbons. Both HETLOC and HSQC-TOCSY experiments rely, in fact, on a 1H - 1H spin-lock magnetization transfer. The homonuclear J couplings were derived, whenever possible, from E-COSY spectra.^[13] In the remaining cases, homonuclear J values were estimated from the DQF-COSY spectra according to the method of Kim and Prestegard.^[14] Additional support for stereochemical assignments came from ROESY^[15] data. In this respect, we found that ROE's could be utilized in this study at two different levels. In fact, proximity contacts between protons within a given C_2 fragment are of crucial importance when a proton-proton *anti* arrangement is present and can generally serve to increase the reliability of relative configuration

Table 1. Dominant rotamers of all sphinxolide (1) C_2 -fragments along with their relative configurations (see also Figure 1); ROESY contacts are classified into strong (s), medium (m) and weak (w) effects

Fragment	Segment	$^3J_{H-H}$ (Hz)	Selected $^{2,3}J_{C-H}$ (Hz) ^[a]	Selected ROE's	Total number of $^{2,3}J_{C-H}$
C32-C33 <i>anti</i> ^[c]		9.0	$^2J_{H32-C33}$ -5.9 (HT and HL) $^3J_{H33-Me32}$ 1.1 (HT and HL) $^3J_{H32-C34}$ 2.6 (HT only)	H34a-Me(m)	4+4 ^[b]
C27-C28 <i>anti</i>		2.4	$^2J_{H28-C27}$ -1.9 (HB) $^3J_{H27-Me28}$ 2.8 (HT only)	H27-Me(s) H26-H29b(m)	4+3 ^[b]
C26-C27 <i>anti</i>		9.8	$^2J_{H26-C27}$ -6.6 (HT and HL) $^3J_{H27-Me26}$ 1.8 (HT and HL) $^3J_{H26-C28}$ 1.5 (HT and HL)	H28-Me(m) H25-OMe27(m)	4+4 ^[b]
C25-C26 <i>syn</i>		1.3 2.6 ^[b]	$^2J_{H26-C25}$ -0.8 (HT and HL) $^2J_{H26-C25}$ -0.9 ^[b] (HB) $^3J_{H25-Me}$ 5.0 ^[b] (HB) $^3J_{H25-C27}$ 2.9 ^[b] (HB)	H25-H27(m) H24-Me(s) H26-H24(m)	4+4 ^[b]
C24-C25 <i>anti</i>		10.0	$^2J_{H24-C25}$ -6.7 (HT and HL) $^3J_{H24-C26}$ 1.5 (HT and HL) $^3J_{H25-Me24}$ 1.4 (HT and HL) $^3J_{H25-C=23}$ 2.8 (HT and HL)	H26-Me(s)	4+4 ^[b]
C20-C21 ^[d] <i>syn</i>		4.4 8.8	$^2J_{H20a-C21}$ -2.8 (HT and HL) $^2J_{H20b-C21}$ -5.6 (HT and HL) $^3J_{H21-C19}$ 2.6 (HT only) $^3J_{H20a-C22}$ 1.8 (HT only) $^3J_{H20b-C22}$ 2.8 (HT only)	H20a-H22(m) H19-OMe(m)	5+4 ^[b]
C19-C20 ^[d] <i>syn</i>		4.4 8.7	$^2J_{H20a-C19}$ -2.2 (HT and HL) $^2J_{H20b-C19}$ -5.1 (HT and HL) $^3J_{H20a-C18}$ 1.0 (HT only) $^3J_{H20b-C18}$ 1.5 (HT only)	H19-H20a(m) H18-H20a(w) H18-H20b(m)	4+4 ^[b]

Table 1 (Continued)

C18-C19 <i>syn</i>		7.2 8.9 ^[b]	$^2J_{H18-C19}$ -5.8 ^[b] (HL) $^3J_{H18-C20}$ 1.0 ^[b] (HL) $^3J_{H19-C17}$ 4.5 (HT and HL) $^3J_{H19-C17} < 3$ ^[b] (HB)	Me-H20a ^[b] (w) H17-H20a ^[b] (w) H17-H20b ^[b] (w)	4+3 ^[b]
C14-C15 ^[d] <i>syn</i>		6.0 ^[b] 15.0 ^[b]	$^2J_{H14b-C15}$ -4.5 (HT and HL) $^2J_{H14b-C15}$ -6.2 ^[b] (HL) $^2J_{H14a-C15}$ -4.8 (HT only) $^2J_{H14a-C15} < -2$ ^[b] (HB) $^3J_{H14b-C16}$ 4.7 (HB) $^3J_{H14b-C16}$ 1.5 ^[b] (HB)	H14b-OMe ^[b] (w)	5+4 ^[b]
C13-C14 ^[d] <i>anti</i>		6.0 ^[b] 8.1 ^[b]	$^3J_{H13-C15}$ 0.9 (HT only) $^2J_{H14a-C13}$ -5.0 (HT only) $^2J_{H14a-C13}$ -5.7 ^[b] (HL) $^2J_{H14b-C13}$ -4.3 (HT only) $^2J_{H14b-C13}$ -9.6 ^[b] (HL)	H12-H15 ^[b] (w) H12-H14b ^[b] (w)	4+4 ^[b]
C12-C13 <i>anti</i>		3.2	$^2J_{H12-C13}$ -1.2 (HB) $^3J_{H13-Me}$ 1.7 (HT and HL) $^3J_{H13-C11}$ 5.0 (HB) $^3J_{H12-C14}$ 0.8 (HB)	Me-OMe(w) Me-H14b(s) H12-H13(m) Me-H13(m)	4+2 ^[b]
C11-C12 <i>syn</i>		10.3	$^2J_{H12-C11}$ -7.7 (HT and HL) $^3J_{H12-C10}$ 1.8 (HT only) $^3J_{H11-Me12}$ 2.9 (HT and HL) $^3J_{H11-C13}$ 1.8 (HT and HL)	OMe13-H10 (w)	4+4 ^[b]
C10-C11 <i>syn</i>		1.1	$^2J_{H11-C10}$ -2.0 (HT and HL) $^3J_{H10-C12}$ 2.6 (HB)	H10-H12 (w)	4
C7-C8 <i>anti</i>		7.0 11.4 ^[b]	$^2J_{H8-C7}$ -5.3 (HT and HL) $^3J_{H8-C6}$ 2.4 (HB) $^3J_{H7-C9}$ 0.7 (HB)	8OMe-H6a ^[b] (s)	4+3 ^[b]

[a] The following short-hand notations have been used: HT = PFG-HSQC-TOCSY, HB = PS-PFG-HMBC and HL = PFG-HETLOC. — [b] J -values and ROEs measured at 276 K. — [c] *anti* and *syn* stereochemical notations have always to be referred to zigzag carbon chains. — [d] According to Murata's paper,^[1] stereospecific methylene protons are referred to as H_a = high field proton and H_b = low field proton. For stereochemical notation purposes, H_b is given higher priority than H_a .

assignments. Moreover, we found that dipolar couplings were also useful in the analysis of spatial relationships of longer carbon sequences, and in many cases provided an independent and more global level of assessment of the three-dimensional features of the system, allowing a cross-check of the stereochemistries already assigned to the individual C_2 units. The dominant rotamers found at 300 K for each C_2 fragment of sphinxolide (**1**), along with their relative configurations, are reported in Table 1.

We must point out that this methodology does not allow the determination of the stereochemical relationships between molecular fragments that are separated by quaternary carbons (or heteroatoms), and therefore our relative configuration assignments are referred to the four C7–C8, C10–C15, C18–C21 and C24–C33 sequences without in-

formation on their relative arrangements.^[16] In selected regions of the molecule, such as the C13–C15 and C18–C19 segments, stereochemical analysis was complicated by a rapid interconversion of different conformers with comparable populations, as indicated by the intermediate value of both homonuclear and heteronuclear coupling constants. As for the C13–C15 moiety, inspection of the spectra acquired at 276 K showed that the population of the dominant conformer was increased up to the point where the method could be safely applied. In particular, when the temperature was lowered from 300 K to 276 K, $^3J_{H14a-H15}$ and $^3J_{H14b-H15}$ changed from the intermediate values of 7.8 and 6.2 Hz to 6.0 and 15.0 Hz, respectively, allowing us to unambiguously establish a *gauche* relationship for H14a–H15 and an *anti* relationship for H14b–H15. Het-

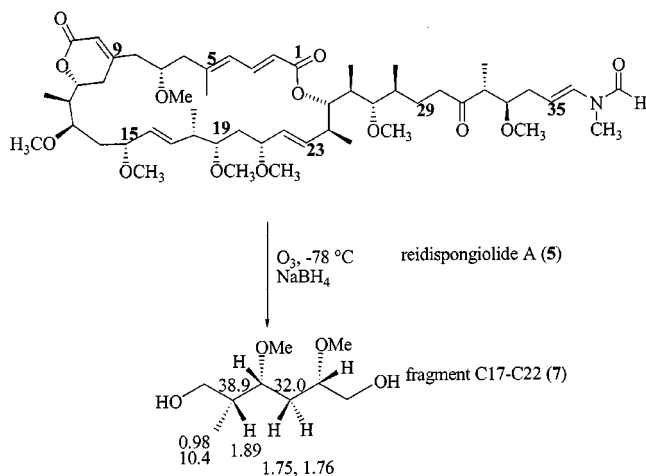


Figure 3. Chemical degradation of reidispongiolide A (5) and selected ^1H and ^{13}C NMR chemical shifts of fragment C17–C22 (7)

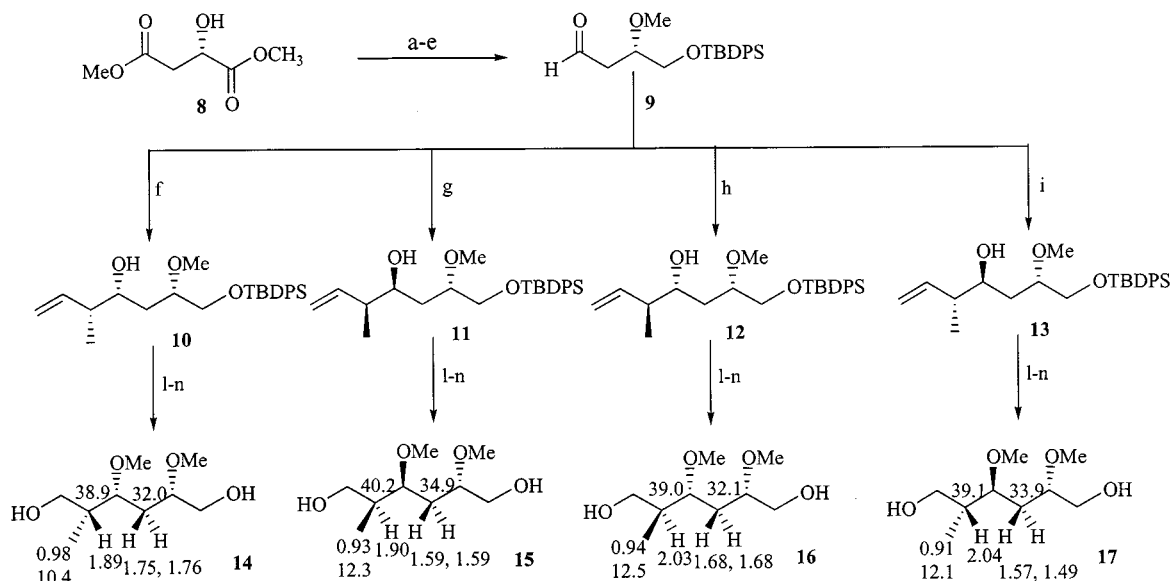
eronuclear J values relative to the same fragment showed a similar behavior. Less clear results were obtained for the C18–C19 unit, where neither the pattern of J couplings nor ROE data (see Table 1) were useful for a stereochemical assignment. Thus, the determination of the configuration of this portion of the molecule had to be addressed by a chemical approach, involving the degradation of the natural product to furnish the segment of interest and the stereoselective synthesis of all its possible stereoisomers. The molecular fragment (7) was prepared from natural reidispongiolide A (5)^[17] by ozonolysis followed by reductive workup (Figure 3).

Scheme 1 summarizes our strategy for the synthesis of all four possible diastereomers of fragment C17–C22 (7). It

involves the use of L-malate dimethyl ester (8) as the chiral starting material and Brown's crotylboration reaction^[18] to provide asymmetric induction and flexibility in constructing the required stereoisomers. The aldehyde 9 was obtained by regiospecific reduction of the L-malate dimethyl ester (8)^[19] followed by conventional functional group manipulation. All the four homoallylic alcohols 10–13 were synthesized by this very efficient reaction simply by varying the stereochemistry of the alkene [(*E*)-2-butene or (*Z*)-2-butene] and that of the chiral auxiliary. A sequence of alkylation, ozonolysis-reduction and deprotection led to the four stereoisomers 14–17 of the C17–C22 fragment.

The ^1H and ^{13}C NMR spectra of the fragment 7 were identical with those of synthetic 14, indicating that the C18, C19 and C21 stereocenters in natural sphinxolide have an all *syn* stereochemistry, as reported in Table 1 and depicted in 1.

In conclusion, we were able to determine the relative configuration of all stereogenic centers of sphinxolide through the application of our HSQC-TOCSY modified version of the J -based NMR configurational analysis and, for a small fragment, by chemical degradation/asymmetric synthesis techniques. As far as the C24–C33 portion is concerned, the relative configurations we found are in agreement with those already reported for related macrolides such as scytopyhins,^[20] aplyronine^[21] and others.^[22] However, the determination of the full stereochemistry of sphinxolides and reidispongiolides still requires the spatial interconnection of the four separate fragments (C7–C8, C10–C15, C18–C21 and C24–C33) and the assignment of their absolute config-



Scheme 1. a) $\text{BH}_3\text{-SMe}_2$ (1.2 equiv.), THF, -78°C , 20 min. then NaBH_4 , 0 – 25°C , 4 h, 90%; b) TBDPSCl, Et_3N , DMAP, CH_2Cl_2 , 25°C , 14 h, 90%; c) $\text{CF}_3\text{SO}_3\text{CH}_3$, di-*t*BuPyr, CH_2Cl_2 , 25°C , 14 h, 87%; d) DIBAL-H, CH_2Cl_2 , -40°C , 2 h, 97%; e) PCC, molecular sieves, CH_2Cl_2 , 1 h, 85%; f) *t*BuOK, (*Z*)-but-2-ene, *n*BuLi, -78 to -45°C , (–)- β -methoxydiisopinocampheylborane, $\text{BF}_3\cdot\text{OEt}_2$, aldehyde 9, -78°C , 4 h, 78%; g) *t*BuOK, (*Z*)-but-2-ene, *n*BuLi, -78 to -45°C , (+)- β -methoxydiisopinocampheylborane, $\text{BF}_3\cdot\text{OEt}_2$, aldehyde 9, -78°C , 4 h, 78%; h) *t*BuOK, (*E*)-but-2-ene, *n*BuLi, -78 to -45°C , (–)- β -methoxydiisopinocampheylborane, $\text{BF}_3\cdot\text{OEt}_2$, aldehyde 9, -78°C , 4 h, 78%; i) *t*BuOK, (*E*)-but-2-ene, *n*BuLi, -78 to -45°C , (+)- β -methoxydiisopinocampheylborane, $\text{BF}_3\cdot\text{OEt}_2$, aldehyde 9, -78°C , 4 h, 78%; l) $\text{CF}_3\text{SO}_3\text{CH}_3$, di-*t*BuPyr, CH_2Cl_2 , 25°C , 24 h, 85%; m) O_3 , CH_2Cl_2 , -78°C , then NaBH_4 overnight, 90%; n) MeOH/HCl 2N, 2 h, room temperature, 90%. TBDPS = *tert*-butyldiphenylsilyl, DMAP = 4-dimethylaminopyridine, Di-*t*BuPyr = 2,6-di-*tert*-butylpyridine, DIBAL-H = diisobutylaluminum hydride, PCC = pyridiniumchlorochromate

uration, two goals that are both currently being pursued in our laboratory.

- [1] N. Matsumori, D. Kaneno, M. Murata, H. Nakamura, K. Tachibana, *J. Org. Chem.* **1999**, *64*, 866–876.
- [2] M. Kurz, P. Schmieder, H. Kessler, *Angew. Chem. Int. Ed. Engl.* **1991**, *30*, 1329–1331.
- [3] J. Boyd, N. Soffe, B. John, D. Plant, R. Hurd, *J. Magn. Reson.* **1992**, *98*, 660–664.
- [4] A. L. Davis, J. Keeler, E. D. Laue, D. Moskau, *J. Magn. Reson.* **1992**, *98*, 207–216.
- [5] P. L. Rinaldi, P. Keifer, *J. Magn. Reson.*, **1994**, Ser. A *108*, 259–262.
- [6] K. E. Kövér, V. J. Hruby, D. Uhrin, *J. Magn. Reson.* **1997**, *129*, 125–129.
- [7] D. Uhrin, G. Batta, V. J. Hruby, P. N. Barlow, K. E. Kövér, *J. Magn. Reson.* **1998**, *130*, 155–161.
- [8] G. Guella, I. Mancini, G. Chiasera, F. Pietra, *Helv. Chim. Acta* **1989**, *72*, 237–246.
- [9] M. V. D'Auria, L. Gomez-Paloma, L. Minale, A. Zampella, J. F. Verbist, C. Roussakis, C. Debitus, *Tetrahedron* **1993**, *49*, 8657–8645.
- [10] X. Zhang, L. Minale, A. Zampella, C. D. Smith, *Cancer Research* **1997**, *57*, 3751–3758.
- [11] M. V. D'Auria, L. Gomez-Paloma, L. Minale, A. Zampella, J. F. Verbist, C. Roussakis, C. Debitus, J. Patissou, *Tetrahedron* **1994**, *50*, 4829–4834.
- [12] Carbonelli, A. Zampella, A. Randazzo, C. Debitus, L. Gomez-Paloma, *Tetrahedron* **1999**, *55*, 14665–14674.
- [13] L. Mueller, *J. Magn. Reson.* **1987**, *72*, 191–196.
- [14] Y. Kim, J. H. Prestegard, *J. Magn. Reson.* **1989**, *84*, 9–13.
- [15] A. Bax, D. G. Davis, *J. Magn. Reson.* **1985**, *63*, 207–13.
- [16] Actually, the side chain fragment C24–C33 contains two subunits separated by the C31 carbonyl functionality. Although the *J*-based method did not provide any stereochemical interconnection between the above subunits, a comparison with several other related marine macrolides would strongly favor the relative configuration depicted in **1**.
- [17] Reidispongiolide A was chosen among all derivatives of the sphinxolide family because it was recently reisolated in large amounts from a recollection of the sponge *Reidispongia coerulesa*.
- [18] H. C. Brown, K. S. Bhat, *J. Am. Chem. Soc.* **1986**, *108*, 5919–5923.
- [19] S. Saito, T. Ishikawa, A. Kuruda, K. Koga, T. Moriwake, *Tetrahedron* **1992**, *48*, 4067–4086.
- [20] M. Ishibashi, R. E. Moore, G. M. L. Patterson, C. Xu, J. Clardy, *J. Org. Chem.* **1986**, *51*, 5300–5306.
- [21] K. Yamada, M. Ojika, T. Ishigaki, Y. Yoshida, H. Ekimoto, M. Arakawa, *J. Am. Chem. Soc.* **1993**, *115*, 11020–11021.
- [22] R. D. Norcross, I. Paterson, *Chem. Rev.* **1995**, *95*, 2041–2114.

Received September 4, 2000

[O00457]